2013

Changing molecular band offsets in polymer blends of (P3HT/P(VDF–TrFE)) poly(3-hexylthiophene) and poly(vinylidene fluoride with trifluoroethylene) due to ferroelectric poling

Freddy Wong
University of Puerto Rico-Humacao, University of Puerto Rico-Rio Piedras

Godohaldo Perez
University of Puerto Rico-Humacao

Manuel Bonilla
University of Puerto Rico-Humacao

Juan A. Colon-Santana
University of Nebraska-Lincoln

Xin Zhang
University of Nebraska-Lincoln

See next page for additional authors

RSC Advances

PAPER

View Article Online
View Journal | View Issue

Changing molecular band offsets in polymer blends of (P3HT/P(VDF–TrFE)) poly(3-hexylthiophene) and poly(vinylidene fluoride with trifluoroethylene) due to ferroelectric poling

Cite this: *RSC Adv.*, 2014, **4**, 3020

Freddy Wong,[ab] Godohaldo Perez,[a] Manuel Bonilla,[a] Juan A. Colon-Santana,[c] Xin Zhang,[c] Pankaj Sharma,[c] Alexei Gruverman,[c] Peter A. Dowben[c] and Luis G. Rosa*[abc]

Received 29th July 2013
Accepted 25th November 2013

DOI: 10.1039/c3ra43993c

www.rsc.org/advances

Photoelectron emission and inverse photoemission spectroscopy studies of polymer blends of poly(vinylidene fluoride (70%) – trifluoroethylene (30%)) P(VDF–TrFE 70 : 30) and regio-regular poly(3-hexylthiophene) (P3HT) provide evidence of changes in the molecular band offsets as a result of changes in the ferroelectric polarization in P(VDF–TrFE). Investigation of the blends with higher concentrations of the semiconducting P3HT component revealed that the organic semiconductor component of the blend dominates the electronic structure in the vicinity of the chemical potential. Specifically, the states of P3HT at the conduction band minimum and valence band maximum fall within the HOMO–LUMO gap of the dielectric ferroelectric P(VDF–TrFE) but the P3HT does not exhibit a change in the molecular band offset with respect to the Fermi level or band bending with polarization reversal, unlike P(VDF–TrFE).

Introduction

Organic semiconductor–ferroelectric blends have the potential for improving organic devices, through more efficient electron hole separation. The recombination of electrons and holes in semiconducting organic polymer blends has been identified as a central cause of energy loss in organic photovoltaic devices (OPV).[1–3] Generally, the main focus of research involving blended organic semiconductor–organic ferroelectric materials centers on the capabilities of the ferroelectric component to hold a permanent polarization in the absence of an external field. The ferroelectric component of the blend, if a permanent polarization is retained, circumvents the need an external bias voltage to efficiently separate the electrons and holes and thus prevent their recombination in photovoltaic devices, especially in organic photovoltaics.

Typically the organic semiconductor is layered, not blended, with a ferroelectric polymer[1–3] or by inclusion of a molecular dielectric layer with a strong intrinsic dipole.[4] The alternating layers of organic semiconductor and strong dipoles in the device structure produce the large, permanent, internal electric field, improving the device performance. The resulting intrinsic electric field, from the organic ferroelectric, is hundreds of times larger than that achievable by the use of electrodes with different work functions. While the details of the ideal multi-layer heterostructure for optimum OPV efficiency are far from certain, the principle has been established. Blends of P3HT/P(VDF–TrFE) may be a good candidate for this application.[3]

The binary ferroelectric polarization physical states, of an organic ferroelectric system, may be used for digital non-volatile memory applications,[5] having the potential for low cost and mechanical flexibility. However, a non-volatile ferroelectric memory device, based on a capacitor read-out of the polarization state, could result in applying a voltage that is larger than the coercive field thus resulting in a rewriting of the polarization state. In order to have a device that does not destroy the polarization and hence the memory state, a different solution for the "read-out" was been proposed by Asadi and coworkers,[5] who developed a storage medium that enables independent read-outs of the polarization and the resistance of the medium. For typical inorganic ferroelectrics, conductivity enhancement is possible, but increased conductivity typically significantly reduces the ferroelectric polarization because the extra charge carriers screen and tend to neutralize the polarization. To address this problem, Asadi and coworkers[5] proposed the combination of organic polymer components that blend semiconducting and ferroelectric properties, specifically poly-(3-hexylthiophene) (P3HT) as the semiconductor, and poly-(vinylidene fluoride with trifluoroethylene) (P(VDF–TrFE)) as the ferroelectric.

[a]*Department of Physics and Electronics, University of Puerto Rico-Humacao, Call Box 860, Humacao, PR 00792, USA. E-mail: luis.rosa13@upr.edu*

[b]*Department of Physics, University of Puerto Rico-Rio Piedras, Call Box 23301, San Juan, PR 00931, USA*

[c]*Department of Physics and Astronomy and the Nebraska Center for Materials and Nanoscience, University of Nebraska-Lincoln, Nebraska 68588-0299, USA*

The role of dipoles and their interfaces in a heterojunction device, using an organic semiconductor (as basic constituent for organic electronics applications), depends on two key issues: charge injection and the molecular band offsets. For many large molecular adlayers, including a number of organic and metal–organic species, the energy level alignment (of the adsorbate) is dependent upon the interfacial electronic structure and the interfacial dipole layer, and has been readily demonstrated for many large molecules, including the metal phthalocyanines.[6–9] Devices that incorporate the polymer blends using ferroelectric components can be used to modulate the injection barrier at the semiconductor to metal contact as well.[6,9] The addition of dipoles or an internal electric field, necessary for significant chemical shifts of the valence band in order to modulate the injection barrier of organic semiconductor metal interfaces, will result in significant changes in the molecular orbitals.[7–9] Since the ferroelectric polymer P(VDF–TrFE) behaves as a wide band gap insulator, it is, nonetheless, still possible to blend an organic semiconductor system with a much smaller band gap. Therefore new bands, due to the organic semiconductor component will be evident in the photoemission spectra, but within the wide band gap of the P(VDF–TrFE). These new bands, associated with the addition of the organic semiconducting P3HT, may appear within the P(VDF–TrFE) but still be placed well away from the chemical potential, both above and below the Fermi level. In this context, states within the gap have been observed with the alkali metal doping of a number of molecular systems with a large gap between the highest occupied molecular orbital (HOMO) and the lowest unoccupied molecular orbital (LUMO),[10–13] indicative of localized states. Such prior work does not establish, however, whether interaction with the molecular host must of necessity pin the conduction and valence band edge to that of the ferroelectric. Our key accomplishment here is that we show that molecular band offsets, due to ferroelectric polarization, may affect only the ferroelectric, not the organic semiconductor.

Experimental

Solutions of regio-regular (RR) poly(3-hexylthiophene) (P3HT) and poly(vinylidene fluoride (70%) with trifluoroethylene (30%)) P(VDF–TrFE 70 : 30) were prepared by dissolving both polymers in tetrahydrofuran (THF). The polymer to polymer mass-concentration ratio of P3HT : P(VDF–TrFE) ranged from 3 : 10, the highest P3HT concentration, to 1 : 10, the lowest P3HT concentration. Ultrathin blends of P3HT/PVDF films of the copolymer 70% vinylidene fluoride with 30% trifluoroethylene, P(VDF–TrFE 70 : 30) and poly(3-hexythiophene) were fabricated by Langmuir–Blodgett (LB) deposition techniques on gold substrates from the water subphase.[14–17] The Au (111) substrates were prepared by thermal evaporation of Au on a mica substrate in vacuum at a background pressure of 1×10^{-7} Torr. The mica (Muscovite mica) had been outgassed at 563 K for 5 hours, and was kept at the same temperature during the gold evaporation. Typically, 100 nm of gold (99.999% purity) was deposited on freshly cleaved mica at the rate of 1 Å s^{-1}.

The polymer blend films were nominally some 10 to 12 molecular layers thick, roughly equivalent to 6 nm thick, as determined by atomic force microscopy (AFM) studies. The films were annealed in ultrahigh vacuum at 110 °C, which has proven to be an effective recipe in prior studies for preparing a clean crystallized ordered surface, and has been demonstrated to result in a surface free from impurities (including water).[18] Poly(vinylidene fluoride) [PVDF, $-(CH_2-CF_2)_n-$] copolymers with trifluoroethylene [TrFE, $-(CHF-CF_2)-$] can form highly ordered crystalline ferroelectric polymer ultrathin films, which has been demonstrated by X-ray and neutron scattering,[14,19–24] scanning tunneling microscopy (STM),[14,16,22,24–30] low energy electron diffraction,[22,27,30] and band mapping.[16,22,27,30] Poly(3-hexylthiophene) can also form highly ordered crystalline semiconductors, as demonstrated though X-ray diffraction by Sirringhaus, Friend and coworkers.[31]

The samples were poled using a macroscopic non-contact probe poling technique, where an electrically biased (in the range of ±900 V) was held at a distance of about 100 μm above the sample surface, as was previously found to be successful for pure PVDF–TrFE films.[32] The ferroelectric polarization orientation was determined by means of piezoresponse force microscopy (PFM) measurements,[32–34] but the "as grown" films are weakly polarized with the dipoles generally oriented up (away from the substrate).[32] Fig. 1 shows the PFM hysteresis loops typical for these regio-regular (RR) P3HT and P(VDF–TrFE 70 : 30). This PFM characterization demonstrates that in spite of blending with P3HT, the films are ferroelectric and retain remanent polarization characteristics of organic ferroelectrics in general.[32–34] Macroscopic poling of the P3HT/P(VDF–TrFE) blended polymer films was carried out by scanning over the entire film area (of the order of 1 cm^2). This non-contact poling technique is a large scale poling of the sample, similar to that used on a more local scale by using various scanning probe microscopy techniques on P(VDF–TrFE 70 : 30) films.[33–44]

The combined ultraviolet photoemission (UPS) and inverse photoemission spectra (IPES) were taken in a single ultrahigh

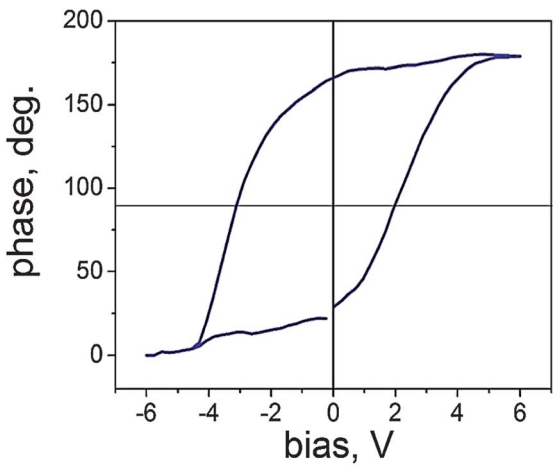

Fig. 1 The ferroelectric hysteresis loop of a Langmuir–Blodgett thin film of RR-P3HT/P(VDF–TrFE) 3 : 10 blend obtained by piezoelectric response microscopy.

vacuum chamber to study the placement of both occupied and unoccupied molecular orbitals of the P3HT/P(VDF–TrFE) polymer blends for a range of different polymer to polymer concentrations, from 3 : 10 (high) to 1 : 10 (low). The IPES were obtained using variable kinetic energy incident electrons while detecting the emitted photons at a fixed energy (9.7 eV) using a Geiger–Müller detector. The inverse photoemission spectroscopy was limited by an instrumental linewidth of approximately 400 meV, as described elsewhere.[6,7,10,11,13,15,16,22,30,32]

The angle integrated photoemission (UPS) studies were carried out using a helium lamp at $h\nu = 21.2$ eV (He I) and a Phi-hemispherical electron analyzer, with an angular acceptance of $\pm 10^\circ$ or more, as described in detail elsewhere.[9,14–16,22,30,32] The photoemission experiments were made with the photoelectrons collected along the surface plane, while the inverse photoemission spectra were taken with the incident electrons normal to the surface. This electron emission (photoemission) or electron incidence (inverse photoemission) along the surface plane was carried out to preserve the highest point group the symmetry and eliminate any wave vector component parallel to surface. In both photoemission and inverse photoemission measurements, the binding energies are referenced with respect to the Fermi edge of gold in intimate contact with the sample surface and the photoemission (obtained by UPS and X-ray photoelectron spectroscopy (XPS)); data are expressed in terms of $E - E_F$ (thus making occupied state energies negative, $E_F = 0$ eV). The core level X-ray photoemission spectra were taken with a VG-Fisons X-ray source with an Al anode ($h\nu = 1486.8$ eV), and a VG 100 hemispherical analyzer, in an ultra-high vacuum chamber also equipped with *in situ* facilities for non-contact poling of the ferroelectric film, as described above. Again, the photoelectrons were collected along the surface plane, and binding energies are referenced with respect to the Fermi edge of gold in intimate contact with the sample surface, thus once again making occupied state energies negative, as binding energies are here written in terms of $E - E_F$.

Theory

Calculations of the molecular orbitals, both occupied and unoccupied, of the polymer blend were performed for purposes of comparison with the density of states deduced from the UPS-IPES experiments. As in previous studies,[6,7,30,32,45–47] the orbital energies of the single molecules (as in a gas phase experiment) were performed with the SPARTAN 10 package, based on density functional theory (DFT), using the conventional B3LYP hybrid functional and the 6–31 G(d,p) basis set, while the semiempirical calculations followed the PM3 methodology. The calculated density of states (DOS) were obtained by applying equal Gaussian envelopes of 1 eV full width half-maximum to each molecular orbital energy to account for the solid state broadening in photoemission, followed by the summing of all envelopes to form the theoretical DOS spectra. These model DOS calculations were rigidly shifted in energy, largely to account for the influence of the work function on the orbital energies, and no correction was made for molecular interactions and final state effects. No corrections were made for matrix element effects or light polarization, and comparison with experiments required caution as both photoemission and inverse photoemission are final state spectroscopies.

The electronic structure of P3HT

Similar to previous combined photoemission and inverse photoemission studies of P3HT,[48,49] we see that the chemical potential of RR-P3HT adjusts to place the Fermi level within the gap, between the HOMO and LUMO, similar to the band offset description for undoped RR-P3HT.[50] The semi-empirical (PM3) calculated density of states, after a rigid energy shift of 5.3 eV to the calculated orbital energies, illustrates good superficial agreement of the combined photoemission and inverse photoemission spectra with expectations, as shown in Fig. 2, consistent with prior work.[48,49] The semiempirical PM3 calculation, shown in Fig. 2b, reproduces the main features of the combined photoemission and inverse photoemission spectra, and, thus, the electronic structure of P3HT, but with several key failings.

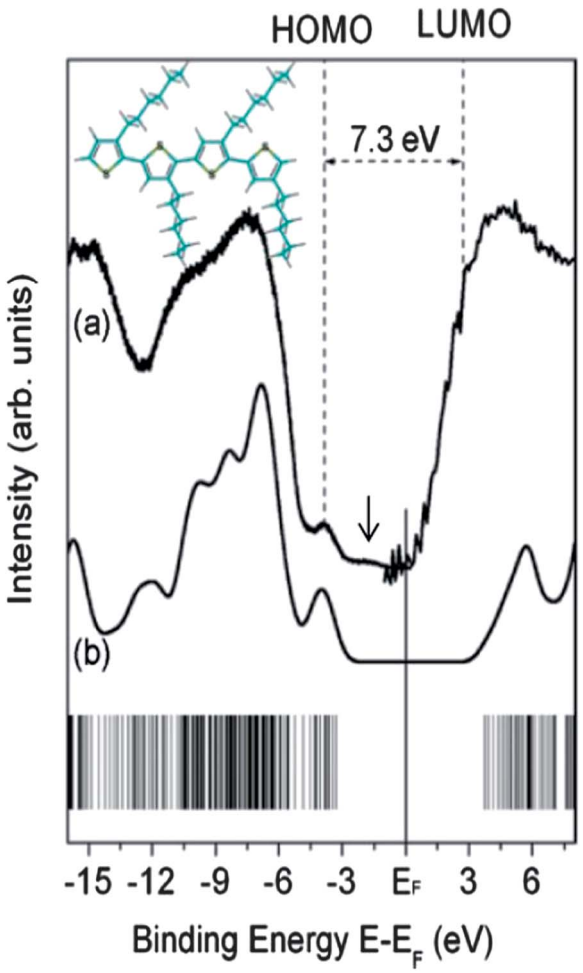

Fig. 2 Electronic structure of P3HT: (a) experimental electronic structure measured by ultraviolet photoelectron emission (UPS) and inverse photoelectron emission (IPES) (b) theoretical density of states (DOS) calculation by PM3 semiempirical methods. Arrow at 1.7 eV on (a) indicates the π electronic contribution to the photoemission spectra.

The exceptions are that some of the occupied density of states (DOS) falls within the gap of the semi-empirical orbital calculation, thus P3HT is more p-type than expected from the comparison with the semi-empirical model calculation. The semi-empirical model calculation suggests a ground state band gap of 7.05 eV, superficially matching the separation of the main occupied and unoccupied molecular orbital features which are separated by 7.3 eV gap (Fig. 2) and similar to the value of 6.4 eV for the HOMO–LUMO gap estimated from the gas-phase XPS on the P3HT monomer.[51] In fact, the agreement between the combined photoemission and inverse photoemission spectra and the semiempirical model calculation is just superficial.

As noted, the very weak feature at a binding energy of 1.7 eV (arrow in Fig. 2a) cannot be assigned to any corresponding molecular orbital in our semiempirical molecular orbital calculations. As shown by Kanai, Seki and coworkers,[52] the band gap for P3HT is much smaller than 7 eV, and the very weak occupied feature at −1.7 eV is a molecular orbital of P3HT, and is reliably reproduced using DFT. This very weak occupied feature at −1.7 eV is dominated by π electrons located on the thiophene rings of the monomers for P3HT, as shown in Fig. 4a. We calculated the band gap of a ten monomer P3HT polymer with DFT (Fig. 3a): the result is a HOMO–LUMO gap of 3 eV, as shown in Fig. 3b, and consistent with prior DFT calculations and experiment.[52] While DFT generally provides a smaller band gap, as is more correct for this molecular system, in fact, the band gap is very sensitive to the RR-P3HT chain length, and also the proximity of adjacent chains, as indicated in Fig. 4.

While the chain length has a significant effect on the band gap, DFT is, in fact, an increasingly accurate description of the combined photoemission and inverse photoemission in part because of the greater solid state effects[45,46] and final state screening.[53,54] The smaller band gap of DFT becomes the more accurate description of the molecular thin film electronic structure only in the systems with a well screened final state. Thus, ascribing the occupied state at a binding energy of −1.7 eV to a defect state, as has been reported,[48,49] is wrong. This photoemission feature is a molecular orbital feature of the P3HT backbone that is actually quite weak because of the weak photoemission cross-section of the HOMO.[52] Indeed both the HOM and the LUMO are dominated by π electrons located on the thiophene backbone.

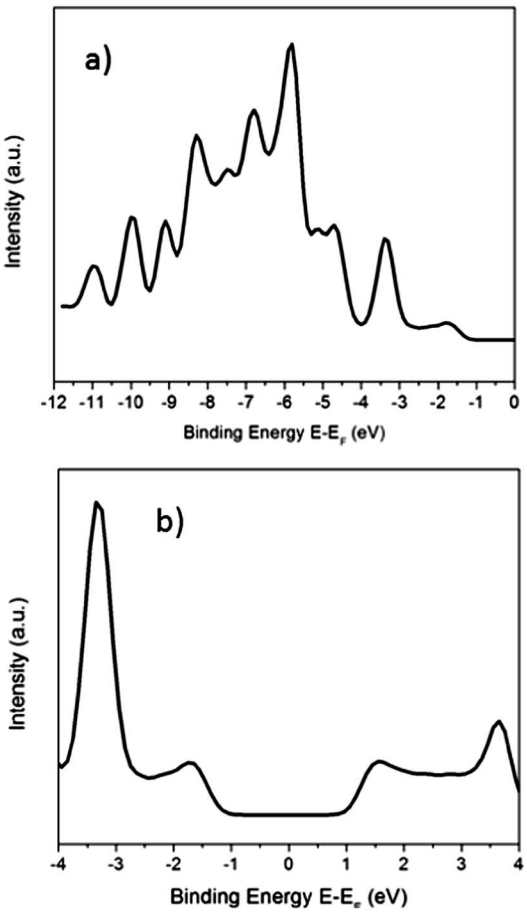

Fig. 3 The P3HT electronic structure density of states (DOS) calculated by density functional theory (DFT). (a) broad spectrum of the calculated valence band region with very good agreement with the experimental spectra from (a). (b) Shows the DOS near the Fermi level, showing a band gap for P3HT of about 3 eV.

The electronic structure of P(VDF–TrFE)

PVDF–TrFE 70 : 30 is not only an organic ferroelectric, but is also a dielectric. As such, final state screening,[54] in photoemission and inverse photoemission is not as significant as in the case of RR P3HT. Thus, the calculated density of states of PVDF–TrFE 70 : 30, by semiempirical methods, together with a rigid energy shift of 5.3 eV applied to the calculated electronic structure, provides a reasonable picture of the electronic structure that is in good agreement with the combined photoemission and inverse photoemission data from P(VDF–TrFE, 70 : 30).[30] The gap between the HOMO and the LUMO, derived from the combined photoemission and inverse photoemission spectra (Fig. 5), indicates that P(VDF–TrFE, 70 : 30) has a band gap of 6 eV.

Electric field poling of the P(VDF–TrFE, 70 : 30) ferroelectric polymer changes the frontier orbitals and termination of the ferroelectric thin film.[32] Thus, poling up (−900 volts to the tip above the grounded sample) results in a hydrogen terminated surface, and poling down (+900 volts to the tip above the grounded sample) results in a fluorine termination. The XPS confirms the increased fluorine surface termination when P(VDF–TrFE, 70 : 30) ferroelectric polymer thin films are poled down. This is evident from the increase in the F 1s core level XPS intensity when poled down in Fig. 5a, in comparison with when the sample is poled up.

The combined photoemission and inverse photoemission spectra of the poled P(VDF–TrFE, 70 : 30) ferroelectric polymer thin film samples are shown in Fig. 6. The apparent larger band gap of the poled P(VDF–TrFE, 70 : 30) ferroelectric polymer thin film sample is similar to that of the unpoled sample, consistent with prior observations that unpoled P(VDF–TrFE, 70 : 30) ferroelectric polymer thin films tend to be poled "up", as grown *via* the Langmuir Blodgett technique (Fig. 6, no poling).[32] The

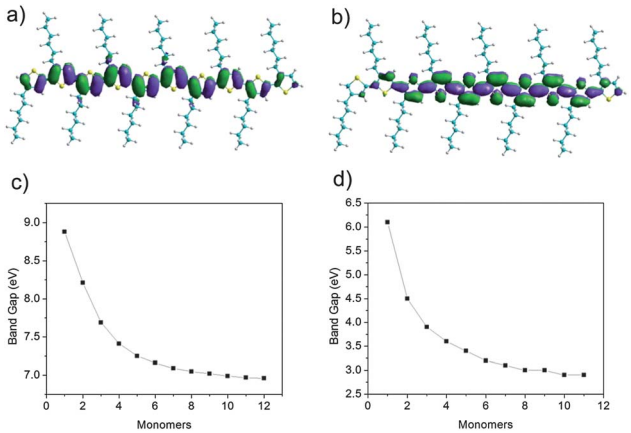

Fig. 4 Band gap orbitals (a) HOMO and (b) LUMO showing π electron orbitals located at the thiophene rings. (c) and (d) show the calculated dependence of the band gap due the increase in the amount of monomers in the P3HT polymer chain. (c) Band gap dependence on PM3 semiempirical calculations and (d) band gap dependence on DTF calculations. DFT yields more accurately the band gap for P3HT system: approximately 3 eV.

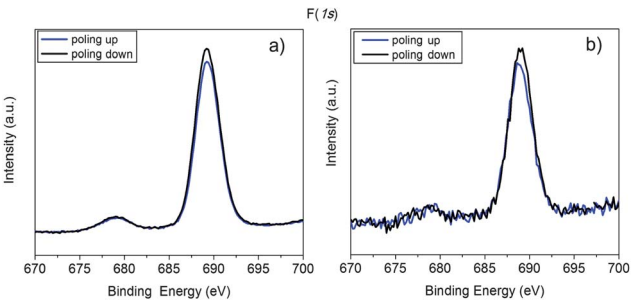

Fig. 5 XPS spectra of the 1s core electron of fluorine atoms in: (a) annealed pristine P(VDF–TrFE) sample and (b) annealed blend 1 : 10 P3HT/P(VDF–TrFE) sample. The photoelectrons were collected normal to the surface. The spectra with the ferroelectric polarization poled up are blue, with polarization down – black.

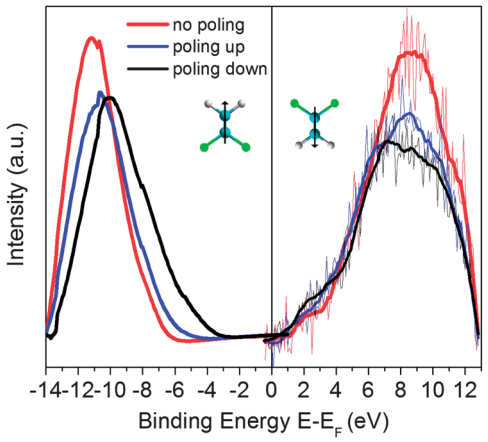

Fig. 6 The experimental electronic structure of P(VDF–TrFE) obtained from the combination of photoemission (left) and inverse photoemission (right), for three different ferroelectric polarization states: (red) non poled sample. The same sample was later poled down (blue) spectra and poled up (black) spectra. Poling was carried out (see text) by applying +900 V with respect to the grounded sample substrate (poled down), and −900 V with respect to the grounded sample substrate (poled up).

change in the molecular band offset, observed between poling up and down, may be as large as 2 eV as shown in Fig. 6, but the P(VDF–TrFE, 70 : 30) ferroelectric polymer thin films are very thin, and poling changes the dielectric properties of these thin films also occur.[25] This latter problem is particularly important in the very thin film limit as the interface P(VDF–TrFE, 70 : 30) layer polarization with the gold substrate is "pinned" in the poled "up" configuration and will not change polarization when the P(VDF–TrFE, 70 : 30) thin film is poled down.[25,55] This leads to significant changes in the conductance and tunneling d(I)/dV curves, with the conductance much lower when the P(VDF–TrFE, 70 : 30) ferroelectric polymer thin films are poled up.[25] As a pragmatic matter, the changes in the experimental electronic structure, due to poling in P(VDF–TrFE), are a combination of a change in the band gap,[53,54] as well as a non-symmetrical rigid shift of the molecular orbitals,[6,56] so that the occupied and unoccupied states appear to behave somewhat differently upon changes in polarization direction. As shown in Fig. 6, poling of the P(VDF–TrFE)–P3HT thin films causes a change in the band gap from 8 eV, with the poling "up", to 6.5 eV with the polarization of the film poled down. This translates to a change in the band gap of about 1.5 eV.

Generally we find that the shift in the valence band edge towards the Fermi level (the placement of the PVDF–TrFE HOMO) is greater (of order 2 eV) in going from poled "up" to poled "down" while for the conduction band edge (the LUMO) there is a rigid shift typically about of 0.5 eV towards the Fermi Level from poling down to up, as shown in Fig. 6 and summarized in the band gap diagram shown in Fig. 7 inset. Thus the change in the molecular band offsets, with a change in the poling direction, are not simply a rigid shift, but somewhat nonsymmetrical between the occupied and unoccupied states. In the blends of P(VDF–TrFE, 70 : 30) the ferroelectric polymer thin film with an organic semiconductor like P3HT, clearly a more complex materials systems, the behavior of the electronic structure with poling is, surprisingly, less complicated.

Evidence of molecular band offset changes in P3HT/P(VDF–TrFE) blends

The combined photoemission and inverse photoemission spectra of the thin film blends of P3HT/P(VDF–TrFE) are shown in Fig. 7, for a high P3HT concentration mass ratio of P3HT : P(VDF–TrFE) of 3 : 10. There is a change in the molecular band offsets of both the conduction band edge and the valence band edge for the PVDF–TrFE component of about 0.5 eV (as indicated by the horizontal arrows in Fig. 7), with different polarization (poling up *versus* poling down) in the blended P3HT/P(VDF–TrFE) films. Unlike with the PVDF–TrFE films, without P3HT, here is a rigid shift to greater or lesser binding energies in the molecular orbital features, characteristic of the changing molecular band offset that accompanies

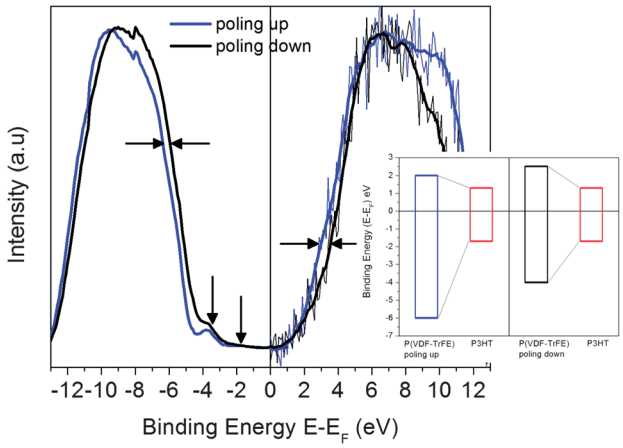

Fig. 7 The combined UPS-IPES spectra of 3 : 10 P3HT/P(VDF–TrFE) for two different poling conditions on the ferroelectric component. Both poling up (black line) and poling down (blue line) spectra show a rigid shift of 0.5 eV. Inset shows the band diagram of P(VDF–TrFE) and P3HT blend. The diagram shows also the HOMO–LUMO gap and their position changes due to poling of the ferroelectric component.

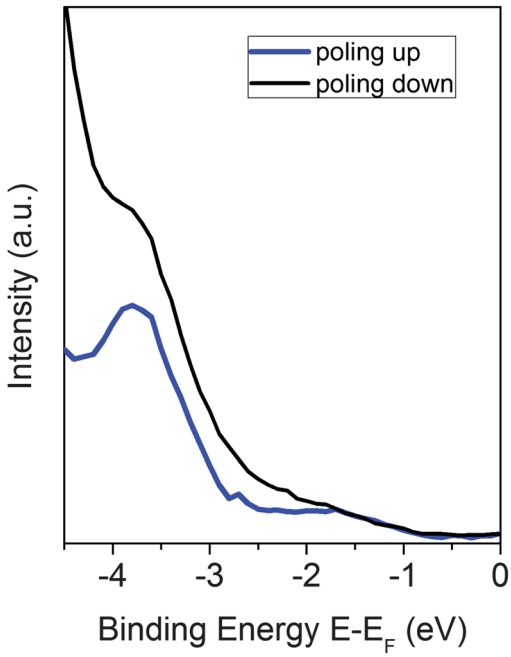

Fig. 8 Combined UPS-IPES spectra of 3 : 10 P3HT/P(VDF–TrFE) for two different poling conditions of the ferroelectric component. The spectral range between 0 and −4 eV clearly shows the features that correspond to the contribution of P3HT to the blend (1.7 eV and 3.8 eV arrows, Fig. 3). Both poling up (black line) and poling down (blue line) spectra show a rigid shift of 0.1 eV.

electron filling or depletion of the molecular orbitals.[7,30,56] With the blend, the shift in the molecular band offset is largely symmetric (Fig. 7), which leads to a superficial simplicity not seem with the PVDF–TrFE films alone (Fig. 6). But unlike ferroelectric–organic semiconductor heterostructures,[6,7,30] the changing molecular band offsets that occur in the blended films only affect the P(VDF–TrFE, 70 : 30), not the P3HT.

Some of the electronic states characteristic of the P3HT component alone can be observed, as they fall within the HOMO to LUMO gap of the P(VDF–TrFE, 70 : 30), in the P3HT/P(VDF–TrFE) thin film blends as is evident from the spectra in Fig. 7 and 8. These characteristic P3HT occupied states (also identified in Fig. 2), are indicated by the vertical arrows located at 3.8 eV and 1.7 eV in Fig. 7. These P3HT weighted states are more clearly evident in Fig. 8, which focuses on the just the occupied states near the Fermi level (largely P3HT) of the P(VDF–TrFE)–P3HT thin film. As just noted above, it is clear that these landmark P3HT features do not shift in binding energy with changing polarization, as evident in Fig. 8. This means that the electronic states at −3.8 eV and −1.7 eV are not affected by the poling of the ferroelectric component P3HT/P(VDF–TrFE) thin film blends. We can thus infer that there is no net change in the extrinsic charge doping of the P3HT component of the P3HT/P(VDF–TrFE) thin film blends, with changing polarization.

The fact there is a changing molecular band offset in the P(VDF–TrFE, 70 : 30) component of the blended P3HT/P(VDF–TrFE) thin film with a change in polarization indicates that the ferroelectric polarization is not completely quenched by the P3HT semiconductor component, consistent with the ferroelectric hysteresis of Fig. 1. The blend must retain some insulating characteristics. While the organic semiconductor does not quench the ferroelectric behavior in the P(VDF–TrFE)–P3HT thin film belnds studied here, because of the addition of the P3HT, the changing molecular band offset in the P(VDF–TrFE, 70 : 30) is clearly distinguishable from any change in the dielectric properties. Metallic conductivity would of course quench any polarization effect altogether, and this does not occur. Because photoemission and inverse photoemission remain surface sensitive techniques, the data must be interpreted cautiously: the changes to the molecular band offsets in the P(VDF–TrFE, 70 : 30) may be just a surface effect, and may not be applicable to the entire film.

Conclusion

The electronic structure of thin film blends of P3HT/P(VDF–TrFE) were characterized by photoelectron emission and inverse photoemission spectroscopies. The electronic structure of the P3HT/P(VDF–TrFE) blends, in the vicinity of the chemical potential (the Fermi level), are in fact dominated by the P3HT molecular orbitals that fall within the HOMO–LUMO gap of the P(VDF–TrFE, 70 : 30) ferroelectric component, as shown in Fig. 7 (vertical arrows). Changing the polarization of the P3HT/P(VDF–TrFE) thin film blended sample does change the molecular band offset of the P(VDF–TrFE, 70 : 30) ferroelectric component, but has little or no effect on the P3HT. The role of dipoles and their interfaces in a heterojunction device that could be fabricated with P3HT/P(VDF–TrFE) has been shown. The dipoles control provided by the ferroelectric component will also influence charge injection and the molecular band offsets. And can be used to modulate the injection barrier due to the ferroelectric component valence band molecular offsets.

Acknowledgements

This work was supported by the Department of Defense Army Research Office Award W911NF-11-1-0184 (proposal # 59012-RT-REP), U.S. Department of Energy, Office of Basic Energy Science, Division of Materials Sciences and Engineering (Award DE-SC0004530), and National Science Foundation through grants NSF-DMR 0923021, NSF-CHE-0909580, NSF-MRI 0923021 and NSF-PHY-1005071, as well as the Nebraska MRSEC (DMR-0820521).

Notes and references

1 Y. Yuan, T. J. Reece, P. Sharma, S. Poddar, S. Ducharme, A. Gruverman, Y. Yang and H. S. Huang, *Nat. Mater.*, 2011, **10**, 296.
2 Y. Yuan, P. Sharma, Z. Xiao, S. Poddar, A. Gruverman, S. Ducharme, J. Huang and Jinsong, *Energy Environ. Sci.*, 2012, **5**, 8558.
3 B. Yang, Y. B. Yuan, P. Sharma, S. Poddar, R. Korlacki, S. Ducharme, A. Gruverman, R. Saraf and J. S. Huang, *Adv. Mater.*, 2012, **24**, 1455.
4 K. Sun, B. M. Zhao, V. Murugesan, A. Kumar, K. Y. Zeng, J. Subbiah, W. W. H. Wong, D. J. Jones and J. Y. Ouyang, *J. Mater. Chem.*, 2012, **22**, 24155.
5 K. Asadi, D. M. de Leeuw, B. de Boer and P. W. M. Blom, *Nat. Mater.*, 2008, **7**, 547.
6 J. Xiao, A. Sokolov and P. A. Dowben, *Appl. Phys. Lett.*, 2007, **90**, 242907.
7 P. A. Dowben, J. Xiao, B. Xu, A. Sokolov and B. Doudin, *Appl. Surf. Sci.*, 2008, **254**, 4238.
8 H. Ishii, K. Sugiyama, E. Ito and K. Seki, *Adv. Mater.*, 1999, **11**, 605.
9 X. Y. Zhu, *Surf. Sci. Rep.*, 2004, **56**, 1.
10 J. Zhang, D. N. McIlroy, P. A. Dowben, H. Zeng, G. Vidali, D. Heskett and M. Onellion, *J. Phys.: Condens. Matter*, 1995, **7**, 7185.
11 P. A. Dowben, D. N. McIlroy, J. Zhang and E. Rühl, *Mater. Sci. Eng., A*, 1996, **217/218**, 258.
12 P. A. Dowben, *Surf. Sci. Rep.*, 2000, **40**, 151.
13 J. Choi, P. A. Dowben, C. N. Borca, S. Adenwalla, A. V. Bune, S. Ducharme, V. M. Fridkin, S. P. Palto and N. Petukhova, *Phys. Rev. B: Condens. Matter Mater. Phys.*, 1999, **59**, 1819.
14 L. M. Blinov, V. M. Fridkin, S. P. Palto, A. V. Bune, P. A. Dowben and S. Ducharme, *Usp. Fiz. Nauk*, 2000, **170**, 247; L. M. Blinov, V. M. Fridkin, S. P. Palto, A. V. Bune, P. A. Dowben and S. Ducharme, *Phys.-Usp.*, 2000, **43**, 243.
15 L. G. Rosa, P. A. Jacobson and P. A. Dowben, *J. Phys. Chem. B*, 2006, **110**, 7944.
16 P. A. Dowben, L. G. Rosa and C. C. Ilie, *Z. Phys. Chem.*, 2008, **222**, 755.
17 G. Xu, Z. Bao and J. T. Groves, *Langmuir*, 2000, **16**, 1834.
18 J. Choi, E. Morikawa, S. Ducharme and P. A. Dowben, *Mater. Lett.*, 2005, **59**, 3599.
19 P. A. Jacobson, L. G. Rosa, C. M. Othon, K. Kraemer, A. V. Sorokin, S. Ducharme and P. A. Dowben, *Appl. Phys. Lett.*, 2004, **84**, 88.
20 L. G. Rosa, P. A. Jacobson, R. Lemoine and P. A. Dowben, *J. Appl. Crystallogr.*, 2004, **37**, 672.
21 L. G. Rosa, P. A. Jacobson and P. A. Dowben, *J. Phys. Chem. B*, 2005, **109**, 532.
22 J. Choi, C. N. Borca, P. A. Dowben, A. Bune, M. Poulsen, S. Pebley, S. Adenwalla, S. Ducharme, L. Robertson, V. M. Fridkin, S. P. Palto, N. Petukhova and A. V. Sorokin, *Phys. Rev. B: Condens. Matter Mater. Phys.*, 2000, **61**, 5760.
23 C. N. Borca, S. Adenwalla, J. Choi, P. T. Sprunger, S. Ducharme, L. Robertson, S. P. Palto, J. Liu, M. Poulsen, V. M. Fridkin, H. You and P. A. Dowben, *Phys. Rev. Lett.*, 1999, **83**, 4562.
24 S. Ducharme, S. P. Palto and V. M. Fridkin, in *Handbook of Surfaces and Interfaces of Materials, Ferroelectric and Dielectric Films*, 2002, 3, 546.
25 H. Qu, W. Yao, T. Garcia, J. Zhang, A. V. Sorokin, S. Ducharme, P. A. Dowben and V. M. Fridkin, *Appl. Phys. Lett.*, 2003, **82**, 4322.
26 L. Cai, H. Qu, C. Lu, S. Ducharme, P. A. Dowben and J. Zhang, *Phys. Rev. B: Condens. Matter Mater. Phys.*, 2004, **70**, 155411.
27 J. Choi, P. A. Dowben, S. Ducharme, V. M. Fridkin, S. P. Palto, N. Petukhova and S. G. Yudin, *Phys. Lett. A*, 1998, **249**, 505.
28 A. V. Bune, V. M. Fridkin, S. Ducharme, L. M. Blinov, S. P. Palto, A. V. Sorokin, S. Yudin and A. Zlatkin, *Nature*, 1998, **391**, 874.
29 S. Palto, L. Blinov, E. Dubovik, V. Fridkin, N. Petukhova, A. Sorokin, K. Verkhovskaya, S. Yudin and A. Zlatkin, *Europhys. Lett.*, 1996, **34**, 465.
30 P. A. Dowben, L. G. Rosa, C. C. Ilie and J. Xiao, *J. Electron Spectrosc. Relat. Phenom.*, 2009, **174**, 10.
31 H. Sirringhaus, P. J. Brown, R. H. Friend, M. M. Nielsen, K. Bechgaard, B. M. W. Langeveld-Voss, A. J. H. Spiering, R. A. J. Janssen, E. W. Meijer, P. Herwig and D. M. de Leeuw, *Nature*, 1999, **401**, 685.
32 Z. Zhang, R. González, G. Díaz, L. G. Rosa, I. Ketsman, X. Zhang, P. Sharma, A. Gruverman and P. A. Dowben, *J. Phys. Chem. C*, 2011, **115**, 13041.
33 P. Sharma, T. J. Reece, S. Ducharme and A. Gruverman, *Nano Lett.*, 2011, **11**, 1970.
34 P. Sharma, D. Wu, S. Poddar, T. J. Reece, S. Ducharme and A. Gruverman, *J. Appl. Phys.*, 2011, **110**, 052010.
35 V. S. Bystrov, I. K. Bdikin, D. A. Kiselev, S. Yudin, V. M. Fridkin and A. L. Kholkin, *J. Phys. D: Appl. Phys.*, 2007, **40**, 4571.
36 S. V. Kalinin, A. N. Morozovska, L. Q. Chen and J. Brian, *Rep. Prog. Phys.*, 2010, **73**, 056502.
37 Y. Kim, W. Kim, H. Choi, S. Hong, H. Ko, H. Lee and K. No, *Appl. Phys. Lett.*, 2010, **96**, 012908.
38 T. Fukuma, K. Kobayashi, T. Horiuchi, H. Yamada and K. Matsushige, *Jpn. J. Appl. Phys.*, 2000, **39**, 3830.
39 K. Noda, K. Ishida, A. Kubono, T. Horiuchi, H. Yamada and K. Matsushige, *Jpn. J. Appl. Phys.*, 2000, **39**, 6358.
40 K. Noda, K. Ishida, A. Kubono, T. Horiuchi, H. Yamada and K. Matsushige, *Jpn. J. Appl. Phys.*, 2001, **40**, 4361.

41 X. Q. Chen, H. Yamada, Y. Teraia, T. Horiuchia, K. Matsushigea and P. S. Weiss, *Thin Solid Films*, 1999, **353**, 259.
42 K. Kimura, K. Kobayashi, H. Yamada, T. Horiuchi, K. Ishida and K. Matsushige, *Appl. Phys. Lett.*, 2003, **82**, 4050.
43 B. J. Rodriguez, S. Jesse, S. V. Kalinin, J. Kim, S. Ducharme and V. M. Fridkin, *Appl. Phys. Lett.*, 2007, **90**, 122904.
44 K. Matsushige, H. Yamada, H. Tanaka, T. Horiuchi and X. Q. Chen, *Nanotechnology*, 1998, **9**, 208.
45 L. G. Rosa, J. Velev, Z. Zhang, J. Alvira, O. Vega, G. Diaz, L. Routaboul, P. Braunstein, B. Doudin, Y. B. Losovyj and P. A. Dowben, *Phys. Status Solidi B*, 2012, **249**, 1571.
46 L. Routaboul, P. Braunstein, J. Xiao, Z. Zhang, P. A. Dowben, G. Dalmas, V. DaCosta, O. Félix, G. Decher, L. G. Rosa and B. Doudin, *J. Am. Chem. Soc.*, 2012, **134**, 8494.
47 L. Kong, L. Routaboul, P. Braunstein, H. G. Park, J. Choi, J. P. Colón Córdova, E. Vega, L. G. Rosa, B. Doudin and P. A. Dowben, *RSC Adv.*, 2013, **3**, 10956.
48 D.-Q. Feng, A. N. Caruso, Y. B. Losovyj, D. L. Schulz and P. A. Dowben, *Polym. Eng. Sci.*, 2007, **47**, 1359.
49 A. N. Caruso, D.-Q. Feng, Y. B. Losovyj, D. Shulz, S. Balaz, L. G. Rosa, A. Sokolov, B. Doudin and P. A. Dowben, *Phys. Status Solidi B*, 2006, **243**, 1321.
50 M. Lögdlund, R. Lazzaroni, S. Stafström, W. R. Salaneck and J.-L. Bredas, *Phys. Rev. Lett.*, 1989, **63**, 1841.
51 M. P. Keane, S. Svensson, A. N. D. Brito, N. Correia, S. Lunell, B. Sjögren, O. Inganäs and W. R. Salaneck, *J. Chem. Phys.*, 1990, **93**, 6357.
52 K. Kanai, T. Miyazaki, H. Suzuki, M. Inaba, Y. Ouchi and K. Seki, *Phys. Chem. Chem. Phys.*, 2010, **12**, 273.
53 L. Kong, G. J. Perez Medina, J. A. Colón Santana, F. Wong, M. Bonilla, D. A. Colón Amill, L. G. Rosa, L. Routaboul, P. Braunstein, B. Doudin, C.-M. Lee, J. Choi, J. Xiao and P. A. Dowben, *Carbon*, 2012, **50**, 1981.
54 J. Xiao and P. A. Dowben, *J. Mater. Chem.*, 2009, **19**, 2172.
55 C. Duan, W. N. Mei, W.-G. Yin, J. Liu, J. R. Hardy, S. Ducharme and P. A. Dowben, *Phys. Rev. B: Condens. Matter Mater. Phys.*, 2004, **69**, 235106.
56 B. Xu, J. Choi, A. N. Caruso and P. A. Dowben, *Appl. Phys. Lett.*, 2002, **80**, 4342.